Towards shape-translational symmetry incommensurate polymer crystals

Mark C. Staub and Christopher Y. Li

Department of Materials Science and Engineering, Drexel University

Philadelphia, PA 19104 USA

Abstract

One of the most interesting characteristics of crystals is their profound morphology. Polyhedron or polygon shapes are often observed in single crystals. The hierarchical structure and morphology of polymer crystals can be described at unit cell, single crystal and spherulite length scales. This article discusses the role of translational symmetry in the evolution of polymer crystal morphology from unit cell to single crystal level. We divide single crystal level crystalline structure into two categories: shape-translational symmetry commensurate crystals (SSCs) and shape-translational symmetry incommensurate crystals (SSICs). The former case includes classical lamellae, dendritic single crystals and epitaxy-driven crystal morphologies. In SSICs, we emphasize crystals' non-flat shapes, which are incommensurate with translational symmetry in Euclidean space. Classical helicoidal, tubular and scrolled crystals are discussed in the context of SSICs. We further highlight the recently discovered spherical crystalsomes which are formed via miniemulsion solution crystallization. This article provides an overview of polymer crystal morphology based on the interplay between crystal shape and translational

symmetry, which may be used to study and design morphologies of semicrystalline polymers and copolymers.

Correspondence author: Chrisli@drexel.edu

Keywords: Polymer crystallization, polymer single crystal, crystalsome.

Introduction

physics.[1-4] The field of polymer crystallization grew and benefited from well-developed understanding of metallurgy and small molecule crystallization.[1-6] Nevertheless, because of polymers' intrinsic long chain nature, polymer crystals and crystallization have brought new insights such as metastability, chain folding, and semicrystallinity to the crystallization field.[1-4, 7-10] Over the years, enormous knowledge, both theoretical and experimental, have been accumulated with regards to all aspects of polymer crystallization, including structure, morphology, and crystallization processes.[1-6, 9] Many exciting developments in the field of polymer crystallization also emerged in recent years, including confined crystallization,[11] theory,[12] crystallization/melting at high cooling/heating rates,[13] crystallization-induced selfassembly,[14-16] functional polymer crystals,[17-27] and crystallization at liquid/liquid

Polymer crystallization is of vital importance in the development of modern polymer

2

interface.[28-32] Confined crystallization is generally defined as the crystallization process

under certain type of geometrical confinement at a small length scale that is comparable to the

chain and/or lamellar dimension.[11] To this end, many intriguing systems have been developed,

including anodized aluminum oxide (AAO) membranes, nanoparticles, polymer nanofibers and

block copolymers.[11] These nano-environments provide limited space for crystals to form; altered crystallization kinetics, crystal orientation, and structures have been reported. Among this, crystallization confined at liquid/liquid interface is a unique subject of study because compared with solid/hard confinement, the dynamic nature of liquid/liquid interface imparts greater mobility of the polymer chain.

Polymer single crystals formed at curved liquid/liquid interface were recently reported. [29, 33, 34] This type of crystals is formed at the interface of mini-emulsion systems, where crystallization is guided by the curved interface, leading to hollow crystalline capsules. Studies have shown that these spherical crystals, named as crystalsomes, show interesting structures and properties. [29, 33, 34] This article will discuss crystalsomes in a framework of translational symmetry in the evolution of crystalline morphology from unit cell to single crystal level. We will first define this framework based on the correlation of crystal shape (morphology) and translational symmetry, and divide the reported polymer crystals into two categories, *i.e.* shape-symmetry commensurate crystals (SSC) and shape-symmetry incommensurate crystals (SSIC). We will briefly comment on selected cases in each category and then elaborate on crystalsomes from the SSIC viewpoint. Future research along this newly developed direction will be discussed. We hope that this framework can provide a guideline for better understanding polymer crystalline morphology in classical and newly developed complex systems.

Crystal morphology and translational symmetry

To understand microstructure of semicrystalline polymers, four levels of hierarchies are typically defined, from chain structures, to unit cells, single crystals, and finally spherulites.

Polymer chain structures, namely detailed chemical structure and regularity of the chains, determine unit cell symmetry (Figure 1). From unit cells to polymer single crystals, following the classical definition, we can first identify a unit cell in a Cartesian coordinate with unit cell parameters of a, b, c, α , β , γ . Translational symmetry can then be applied, i.e. the unit cell is translated along the three axis directions by integer times of the unit cell lengths and the resultant structure is identical to the original one. Unit cell and translational symmetry are the most basic aspects of crystals. When moving from unit cell level to a larger length scale, surface free energy-dictated crystal growth rates along different crystallographic directions, combined with the intrinsic unit cell symmetry, lead to faceted polymer single crystals that have been widely observed. When materials supply is limited, diffusion becomes an important factor for crystal morphology development and various types of dendritic and fractal-type crystals are formed. In all these cases, translational symmetry is held in single crystals even when the crystal facets are not well-defined. These crystals can be considered as SSCs since their morphology and translational symmetry are commensurate and translation symmetry can be applied in the entire crystalline domain.

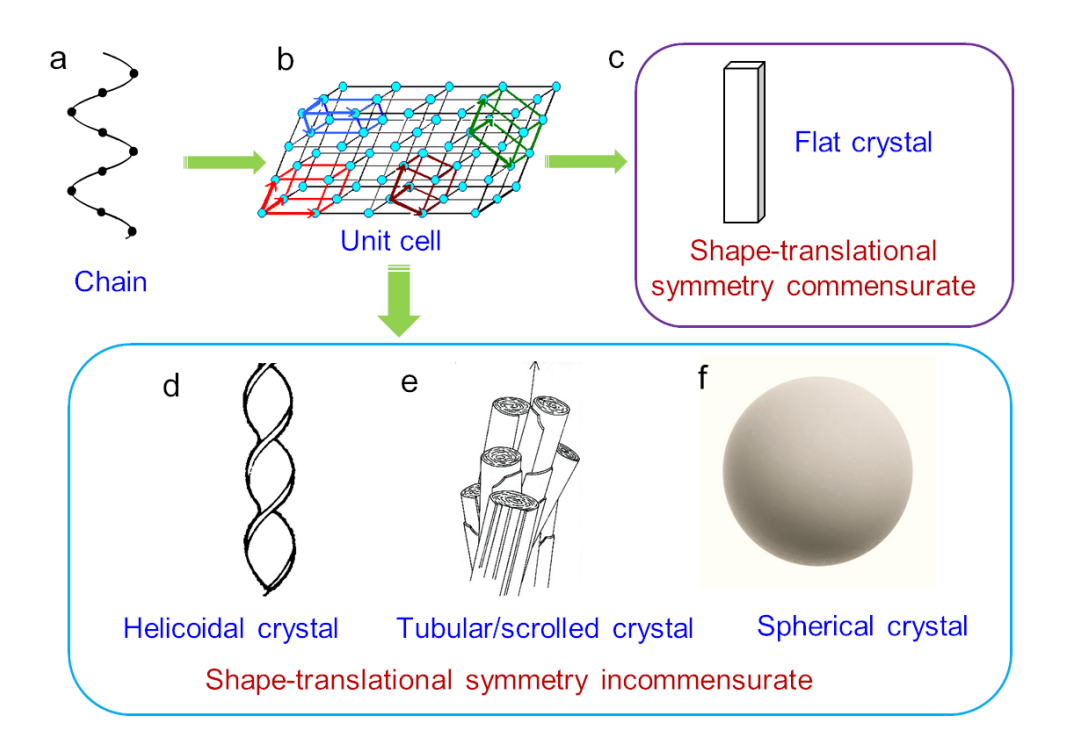


Figure 1: Hierarchical structure and translational symmetry in polymer crystals. (a) Chain structure. (b) Unit cell structure. (c) Flat shape-translational symmetry commensurate crystals. (d-f) Non-flat shape-translational symmetry incommensurate crystals with (d) helicoidal, (e) scrolled and (f) spherical shapes.

In SSICs, morphology of the crystal dictates broken translational symmetry along at least one-unit cell axis. Since unit cells are defined based on a Cartesian coordinate, SSICs are typically observed in non-flat crystals; examples are helicoidal, helical, tubular, scrolled and bowl-shaped lamellar crystals (**Figure 1**). **Table 1** lists a few typical morphologies and their corresponding characteristics. Note that the discussion on SSICs is focused on the translation from unit cell to single crystal level structures. At the spherulite level, as spherical symmetry dominates the microstructure, within one spherulite, the radial direction has the same crystallographic axis, therefore translational symmetry is broken. This type of translational

symmetry breaking is associated with non-crystallographic lamellar branching as they form and will not be discussed in this article.

Table 1. Crystal morphology defined based on the morphology-translational symmetry commensurability.

Crystal	Morphology	Translational symmetry	Comments
SSC	Shish/ribbon/lamellae	3D	Classical single crystals
	Dendritic single crystal	3D	Translational symmetry is held in these crystals even though crystalline facets are not evident
	Memory effect in polymer single crystals	3D	Orientational control in self-seeded crystal growth
	Epitaxy-driven morphology	3D	Translational symmetry dictates morphology development through materials interfaces. Programmable growth of crystal and assembly
SSIC	Helicoidal-single twist	1D	Single twist packing
	Helicoidal-double twist	No	Double twist packing
	Scrolled/tubular	1D	Unbalanced fold surface is the main driving force for symmetry breaking
	Bowl	No	Unbalanced fold surface is the main driving force for symmetry breaking
	Spherical crystalsome from emulsion crystallization	No	Templated and confined growth

Classical polymer single crystals exhibit 1D or 2D morphology with well-defined translational symmetry. In 1D, well-known morphologies include fibrous crystals and ribbons. Extended chain conformation can be found in typical fibrous crystals such as shish formed in flow-induced crystallization. Many conjugated polymers form 1D anisotropic ribbons where

polymer chains are perpendicular to the ribbon axis, and fold surface is along the ribbon long axis. Polyethylene (PE) typically crystallizes into the most abundantly observed 2D lamellar crystals; sectors are observed with different fold directions as shown in Figure 2a,b,[35] where PE decoration demonstrates different folding direction in the four sectors and the selected area electron diffraction (SAED) pattern shows single orientation of the crystal lattice. Solution grown PE single crystals adopts a 3D pyramid shape, revealed in Figure 2c,d.[36] Despite the 3D shape and sectorization of the crystal, translational symmetry is retained in the crystalline domain of the crystals. Beyond these classical single crystal morphologies, the important role of translational symmetry in determining the crystal structure and morphologies can be further illustrated in three unconventional cases: 1) Thin film crystallization where diffusion affects the final crystal morphology and dendritic like single crystals can be observed. Figure 2e shows a dendritic single crystal obtained in poly(2-vinylpyridine)-b-poly(ethylene oxide) (P2VP-b-PEO).[37, 38] 2) Orientation control in self-nucleated polymer crystals. Crystal lattice orientation can be retained even in the molten phase that is not far above the crystal melting temperature. When cooled, multiple small crystals are formed in a mother lamella domain with the same orientation, the so-called cloning effect (Figure 2f,g).[16] These individual crystals show the original crystal orientation and translational symmetry again is kept among these newly formed crystals. 3) While 2D lamellae are the dominant shape in polymer single crystals and fold surface are known to be nanocrystalline, it has been found that the overgrown crystals on the fold surface often have the same lattice orientation compared with the original lamellae. Figure 2h shows a phase contrast microscopy image of a polycaprolactone (PCL) single crystal film formed on water surface. [28] Because of the slow evaporation process, the single crystal can reach centimeter lateral size with one single lattice orientation (SAED pattern is shown in the

inset). Interestingly, the overgrown PCL single crystals have a hexagonal shape and they are all aligned in one orientation templated by the underneath single crystals. Therefore, translational symmetry is retained in adjacent layers. Tie chains between the adjacent lamellae or surface roughness of the lamellar surface may play a pivotal role in this type of symmetry translation.

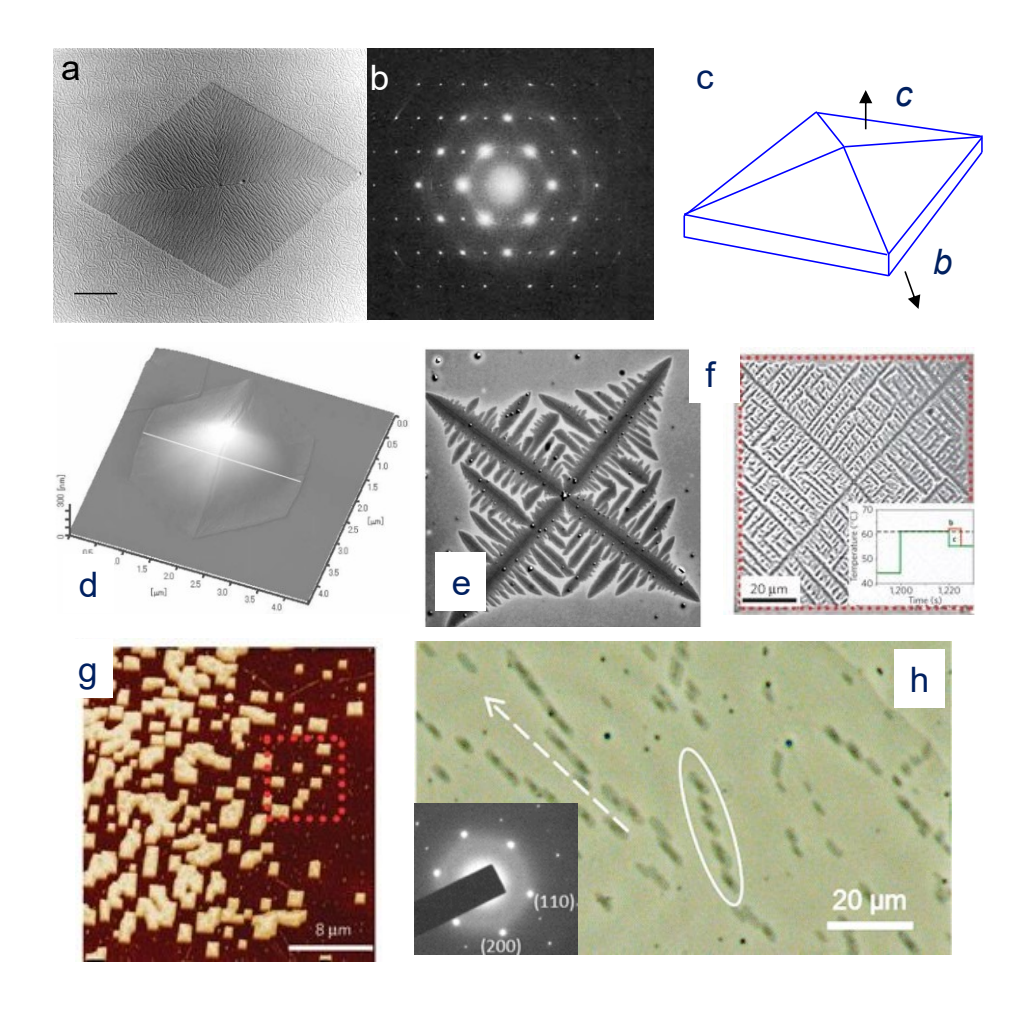


Figure 2. Examples of shape-translational symmetry commensurate polymer crystals. (a) 2D PE single crystals decorated with PE oligomer rods, and (b) the corresponding selected area electron diffraction patter.[35] (c) Schematic representation of a hollow pyramid PE single crystal and (d) AFM image of a 3D PE single crystal.[36] (e) Optical micrograph of a dendritic single crystal of P2VP-*b*-PEO.[37] (f-g) Transforming of a large dendritic single crystal of P2VP-*b*-PEO into a uniquely oriented small crystal.[16] (h) Phase contrast image of a large PCL single crystal film

with overall grown hexagonal PCL single crystals with well-defined orientation. Inset shows the corresponding electron diffraction pattern.[28]

Another group of structures that is dictated by translational symmetry is epitaxy-based crystalline morphologies. Epitaxy has been extensively investigated and lattice matching in epitaxial growth can be viewed as following translational symmetry because the orientation of the secondary structure is dictated by the first one with a pre-determined orientation.[39, 40] In addition to the classical epitaxial growth cases for nucleation agent selection, epitaxy-driven growth has been recently used to fabricate numerous functional polymer assemblies. For example, crystalline polymers with different chain end groups have been programed to grow in one single crystal with a single lattice orientation.[18] The programmed chemical functionality allows one to patten nanoparticles in a well-controlled fashion (Figure 3a).[18, 41] Figure 3a shows the schematic representation of the programable growth of thiol-poly(ethylene oxide) (HS-PEO) single crystal. By controlled addition of gold nanoparticles (AuNPs), these PEO single crystals can be used as the template to pattern AuNPs. By controlling the chain end groups and programing the crystal growth, different kinds of nanoparticle can be patterned on one single crystal as showing in Figure 3c,d. Free-standing AuNP frames can also be synthesized when poly-4-vinylpyridine-block-poly(ethylene oxide) (P4VP-b-PEO) is used to guide the AuNP assembly and for nanoparticle crosslinking (Figure 3e,f).[41] Since polymer single crystals can be used as the template to synthesize polymer brushes with controlled grafting density, [42, 43] programing growth with controlled translational symmetry leads to precisely patterned and gradient polymer brushes (**Figure 3g,h**).[44] Epitaxy also plays a vital role in the recently developed study on crystallization-induced self-assembly, where semicrystalline polymers are

used as one block of a block copolymer. Using similar programmable growth, a variety of patterns have been successfully obtained.[45, 46]

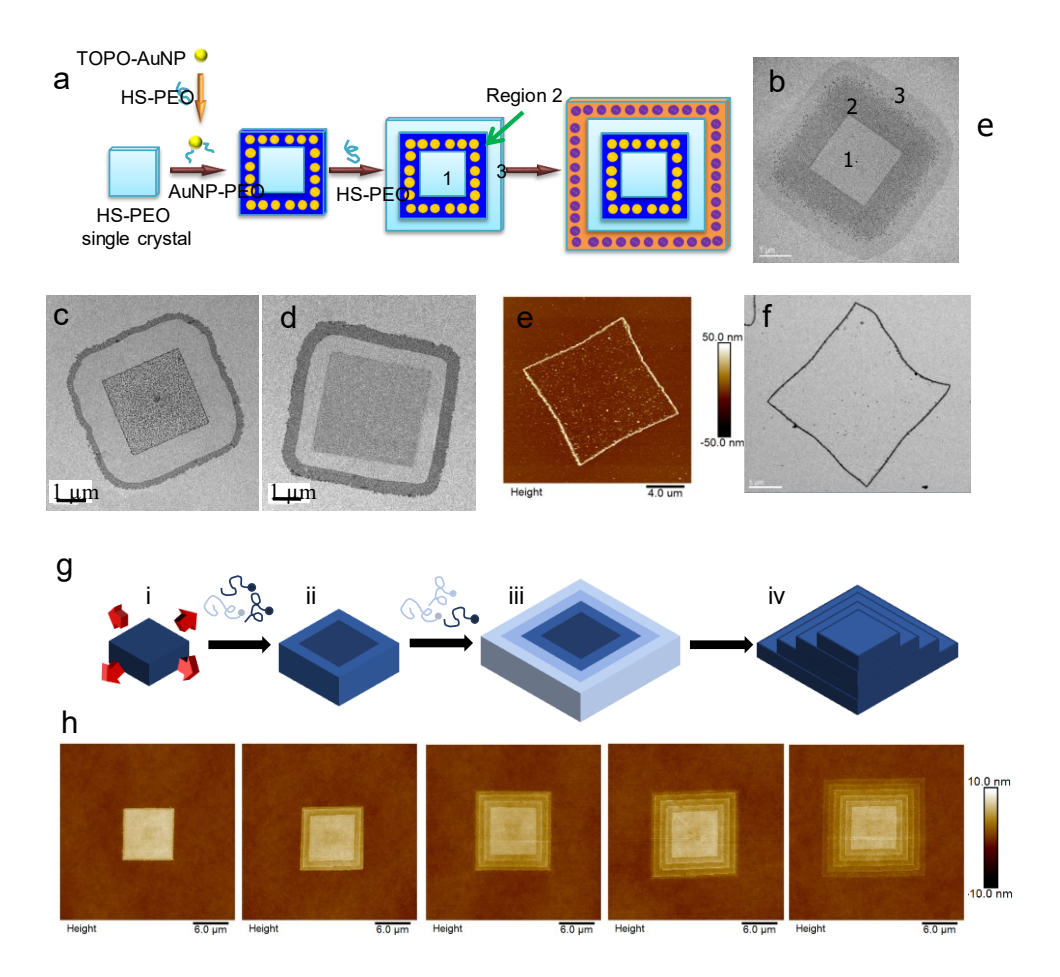


Figure 3. Translational symmetry in programmable growth of functional polymer single crystals.

a) Schematic representation of programmable patterning AuNPs on HS-PEO single crystal surface. (b-d) Shows PEO single crystals decorated with AuNP, AuNP/magnetite NP and AuNP/CdSe@ZnS.[18] (e-f) are AFM and TEM images of free-standing AuNP nanorings that mimic cyclic polymers.[41] (g) Schematic representation of PEO single crystal-templated gradient polymer brushes, and (h) shows a series of AFM height images of the fabricated gradient polymer brushes.[44]

One noteworthy study is on soft epitaxy, which is defined in carbon nanotube (CNT)-induced polymer crystallization.[47, 48] Due to the small diameter, when CNT-induced polymer crystallization occurs, polymer crystal growth does not strictly follow molecular lattice matching. Instead, polymer chains tend to align parallelly to the CNT axis disregarding its detailed lattice orientation (**Figure 4a**, right). This leads to the widely observed hybrid shish kebab structure.[24, 47-51] If we consider multiple kebab crystals in a hybrid shish kebab, their *c* axes have the same orientation due to translational symmetry templated by the CNT (**Figure 4a**). Therefore, 1D nucleated shish kebab structure can be considered as epitaxy-driven morphology. Note that the soft epitaxy is size dependent in CNT-induced crystallization; when large diameter carbon nanofibers are used as the nucleation agent, lamellae with multiple orientation was observed because lattice epitaxy becomes the dominant growth mechanism. Block copolymer PE-*b*-PEO has also been used to crystallize on CNT surface. Well controlled periodic patterns were formed, which was driven by CNT-induced polymer crystallization.[52]

Recent work has extended this observation to polymer nanofiber-induced crystallization.[53-59] Nanofiber shish kebabs have been observed in a number of systems such as PCL and PEO nanofibers. Most recently, poly(lactic acid) (PLA) nanofiber shish kebabs containing stereocomplex crystal (SC) shish and SC/homocrystal (HC) kebabs have been.[57] **Figure 4c** shows the schematic representation of the SC nanofiber shish kebab formation process and the corresponding SEM image. PLA SC kebab lamellar crystals are uniformly formed on the PLA SC shish. Translational symmetry is retained in all kebabs, rendering the parallel orientation of the kebab crystals. We also reported that when block copolymer PCL-*b*-poly(acrylic acid) (PCL-*b*-PAA) is used to form kebabs on PCL nanofiber, the block copolymer nanofiber shish kebabs can be used as the template for the formation of biominerals such as

hydroxy apatite (HA).[55] This unique design provides both spatial and orientational control of HA nanocrystal formation on an organic fiber template, mimicking natural bone structure.

Figure 4d shows the schematics of the design and an SEM image of mineralized nanofiber shish kebabs. HA crystal formation can be confirmed by SAED and 2D wide-angle X-ray diffraction (WAXD) experiments. The c axis of the HA nanocrystals is perpendicular to the fiber axis, controlled by the translational symmetry among the parallel kebab crystals.

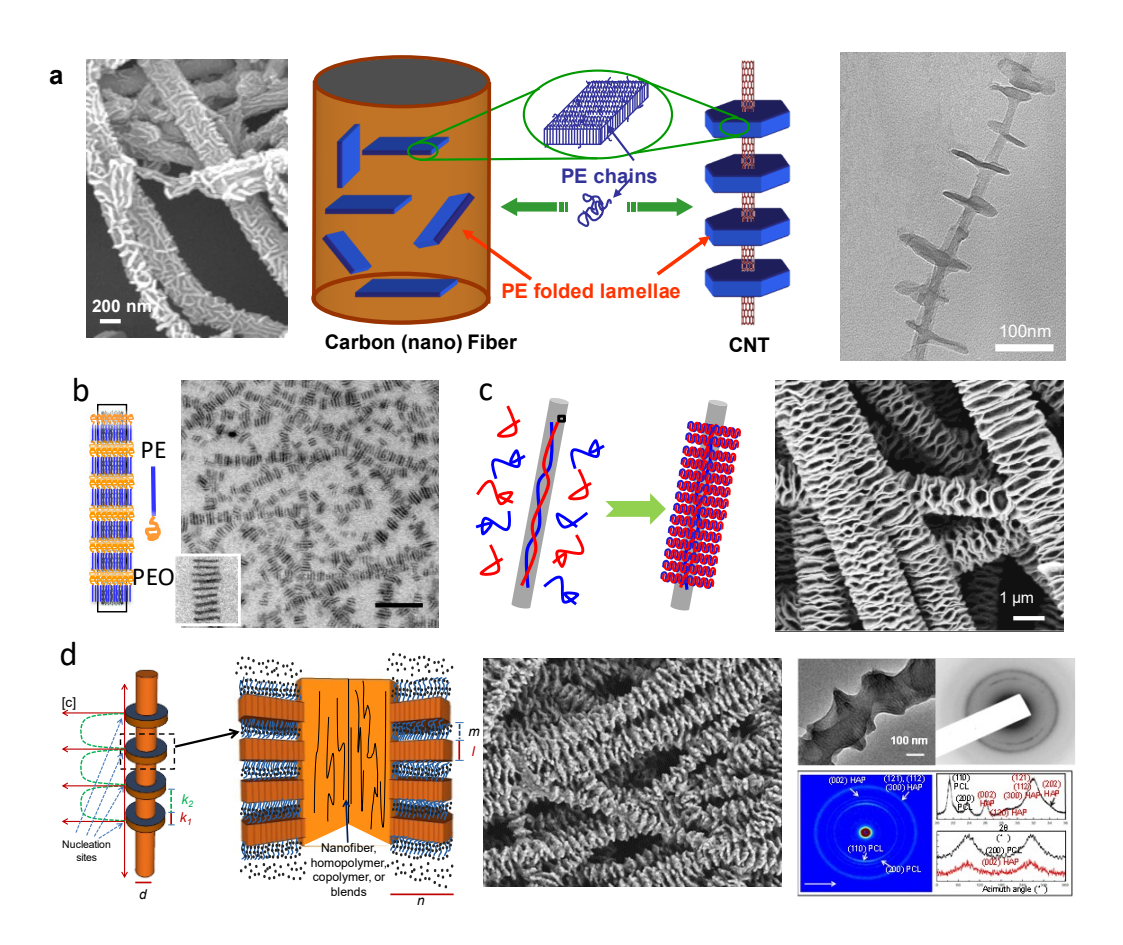


Figure 4. Soft epitaxy-driven morphology in shish kebabs. (a) Shows the size dependent soft epitaxy mechanism in CNT-induced polymer crystallization.[48] (b) CNT-induced PEO-*b*-PE crystallization.[52] (c) Shows the schematic and an SEM image of nanofiber shish kebabs where

PLLA/PDLA blends are used as the shish and kebab polymers.[57] (d) Illustrates when PCL is used for shish nanofiber and PCL-*b*-PAA for the kebab crystal, the block copolymer kebabs can be used as the template for biomineralization. SEM, TEM and 2D WAXD characterization of the mineralized nanofiber shish kebabs is shown in the figure.[55]

Shape-translational symmetry incommensurate polymer crystals

Non-flat morphology is a common characteristic for SSICs and it can form spontaneously upon crystallization, or, templated by an external nano-environment. The most extensively studied polymer SSICs are helicoidal lamellae which are observed in banded polymer spherulites or in single crystals formed in several reported systems. [60, 61] Figure 5a,b shows the SEM image and schematic representation of PE spherulites with twisted lamellar crysatls. The origin of the helicoidal structure in polymer spherulites has been long debated and according to Keith and Pattern, unbalanced stress associated with tilted chains with respect to the lamellar fold surface is the driving force for the observed lamellar twisting. [60, 61] Other mechanisms such as isochiral screw dislocations, [62] self-induced compositional or mechanical field at the crystal growth front, [63] rhythmic crystallization from nonlinear diffusion of the molecules, [64] and topological defects in finite crystalline ribbons have also been proposed to explain lamellar twist and banding in spherulites. The continuous twist structure has been illustrated on a single crystal level and also monitored using microbeam synchrotron X-ray diffraction. [65] By sampling 2D WAXD and small angle X-ray scattering (not shown) patterns of the PE spherulite along the radial direction, intensities of the diffraction peaks were plotted against the radial location

(**Figure 5c,d**). The periodic change of the diffraction intensity confirms the twisted crystal morphology. Helicoidal crystals in other nonchiral or chiral polymers have also been extensive studied.[60]

Well-defined helicoidal single crystals were observed in a series of chiral main chain liquid crystals (**Figure 5e-I**). Continuous lamella twist is clearly seen. Two types of chain twisting geometries were defined, *i.e.* single twist and double twist. For single twist, there is only one twist axis which is along the helical axis. For double twist, chain lattice twists along both the long and short axis of the helicoidal crystal (**Figure 5f, g**). Combined TEM SAED and dark field imaging experiments demonstrated that lattice twists along both the helical and transverse directions, and the double twist model was therefore confirmed in this series of crystals.[66-72] Such double twisted structure suggests that translational symmetry is broken in all directions. While chirality was believed to be important for determining the twist sense and breaking of the translational symmetry, it was found that crystallization condition as well as the spacer length are equally important, highlighting the complexity of the translation symmetry evolution.

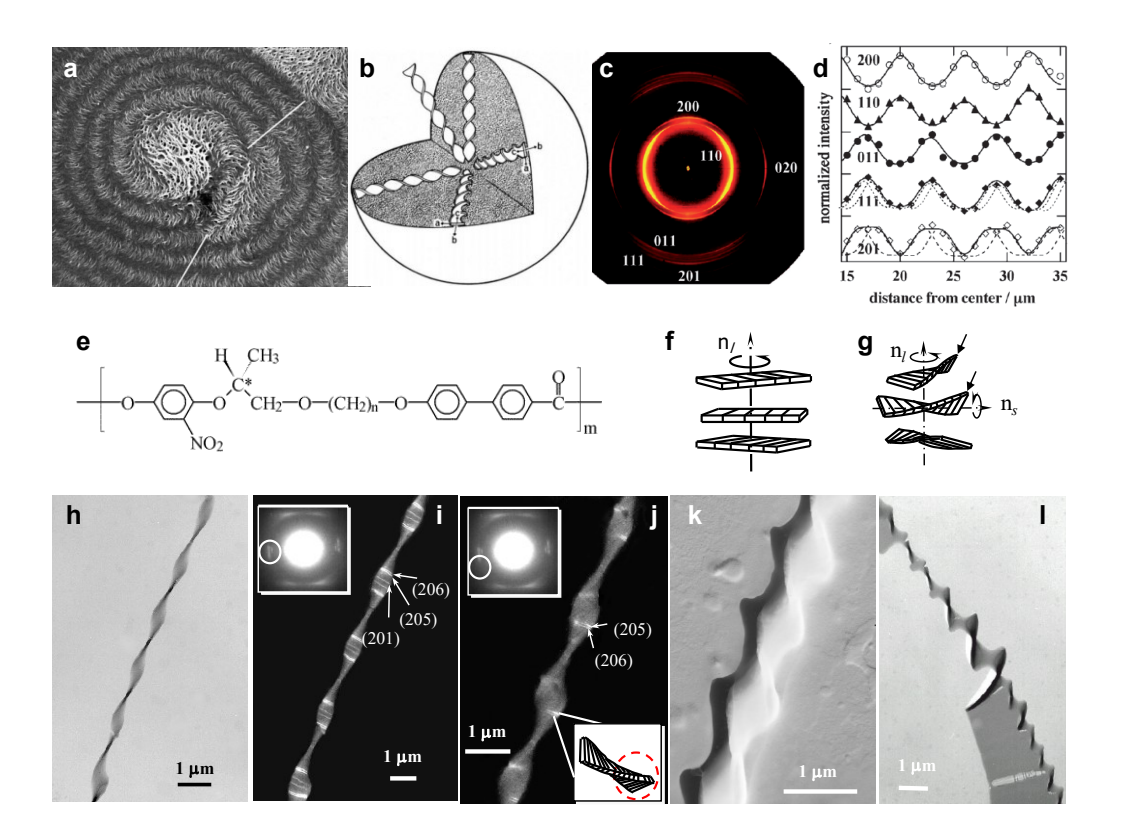


Figure 5. Helicoidal crystals as shape-translational symmetry incommensurate polymer crystals. (a-b) are SEM image and schematics of banded PE spherulites.[60] (c) microbeam 2D XRD pattern of a PE spherulite. (d) shows the lamellar orientation change as the X-ray beam moved along the radial direction, confirming lamella twist.[65] (e-i) illustrate helicoidal crystals formed in a series of main-chain chiral liquid crystals (e). (f-g) show the single-twist (f) and double-twist (g) geometry.[66] Combined TEM bright field (f) and dark field (i-j) experiments confirm the double-twist nature.[66] The nature of translational symmetry breaking is associated with lamellar twist. Interestingly, right-handed twist was observed for n=9 while left-handed twist was observed for n=10 (k).[68] Flat and helical crystals can coexist in one single crystal (l).[69]

Another type of non-flat SSICs with broken translation symmetry possess a tubular or scrolled morphology. Examples are poly(amide 6,6) (PA66) and poly(vinylidene fluoride)

(PVDF) γ phase crystals. In PA66, scrolled/tubular single crystals were observed using solution crystallization with a tube diameter of ~ 350 nm (Figure 6a).[73, 74] Interestingly, the formation of this non-flat crystal morphology was correlated with self-seeding temperature, suggesting that the driving force of the scrolled crystal with broken translational symmetry is due to the imbalance of the folded basal surface of the lamellae: as shown in figure 6b, the folding is symmetric when either acid or amine folding is formed in flat PA 66 single crystals (**Figure 6b**). When both acid and amine folding are formed and each folding structure is located on one side of the lamella (Figure 6c), the folding is asymmetric with unbalanced fold surfaces, leading to the observed PA66 crystal scrolling.[73] It was recently reported that scrolled crystals are closely associated with the negatively birefringent PA spherulites.[74] In PVDF, microscrolls were first observed on the surface of γ PVDF (**Figure 6d**).[75] Lotz *et al.* rationalized that these scrolls are the building blocks of y PVDF spherulites, and the formation of the scrolls was attributed to the volume mismatch of the opposite fold surfaces of the PVDF lamellae.[60] Individual γ PVDF scrolls were recently observed using solution crystallization and it was found that these scrolls have a diameter of $\sim 310-520$ nm. Translational symmetry is retained along the scroll axis (b) (Figure 6e).[76] Bowl-shaped crystals are another type of SSICs, which have been reported in a triblock copolymer polystyrene-b-poly(ethylene oxide)-b-poly(1-butene oxide) (PS-b-PEO-b-PBO).[77] Upon PEO crystallization, PS and PBO separate into top and bottom surfaces of the PEO single crystal, leading to crystal bending. Translation symmetry is broken in all direction in the bowl-shaped space.

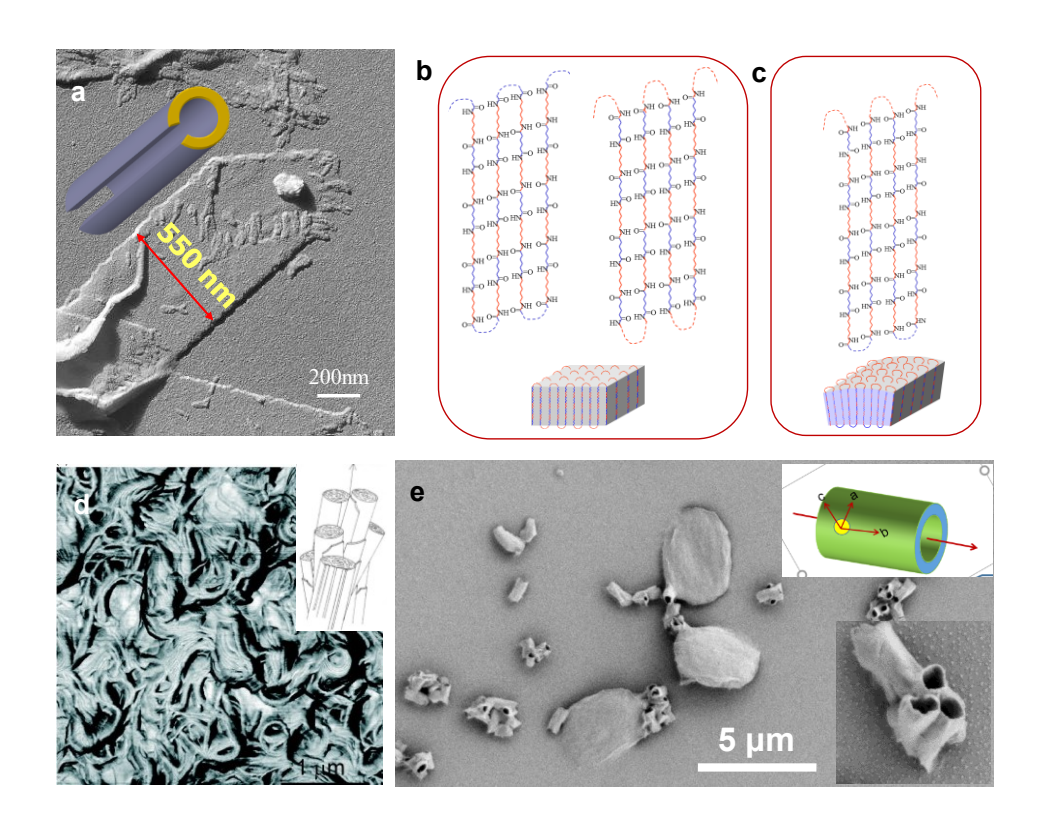


Figure 6. Scrolled single crystal as shape-translational symmetry incommensurate polymer crystals. (a) TEM image of a scrolled PA 66 single crystal. (b-c) show symmetry folding and asymmetric folding of PA 66 chains in the crystal.[73] (d) AFM and (e) SEM images of PVDF scrolled spherulites (d) and single crystals (e).[60, 76]

Polymer crystalsomes

Polymer crystalsomes, formed by miniemulsion crystallization, represent a recently discovered SSICs. A typical crystallization process includes 1) formation of a miniemulsion system where nanosized emulsion droplets are comprised of crystallizable polymers and organic solvent, 2) quenching the emulsion system to a crystallization temperature where liquid/liquid phase separation within the droplet is avoided (**Figure 7a,b**).[29] It is anticipated that one single crystal nucleus formed in each droplet and the nucleus will be pinned at the liquid/liquid

interface according to the Pickering emulsion mechanism. The curved interface can then guide single crystal growth. After filling the curved liquid/liquid interface with 2D lamellar crystals, crystalsomes are formed (Figure 7a). The name crystalsome was derived from similar assembly structures such as polymersome or liposome. Different from polymersomes which are formed due to self-assembly of amphiphilic block copolymers, the formation of crystalsomes is driven by crystallization of polymers at curved liquid/liquid interface. Both homopolymers (such as poly(L-lactic acid), PLLA and PE) and block copolymers (such as PLLA-*b*-PEO) have been used to form crystalsomes. Figure 7d-g shows TEM bright field images, an SAED pattern and a reconstructed tomography TEM image of PLLA crystalsomes. Single crystal-like diffraction pattern can be seen. Note that this is due to the gradual change of lattice orientation during crystal growth (Figure 7h) and SAED only arises from a small portion of the area on a crystalsome surface. (hk0) SAED arcs become broader as the crystalsome diameter decreases (Figure 7d-g), suggesting more significant splaying of the lattice as crystalsome curvature increases.

The formation process of crystalsomes in emulsion crystallization can be viewed as confined crystallization. Since the crystals have a hollow spherical shape, and SAED showed that polymer chains are perpendicular to the lamellar surface (**Figure 7d-g**), translational symmetry therefore is broken in the entire spherical crystal. This is different from other nanoconfined crystallization. Considering a nanodroplet (either in block copolymer case or an emulsion system where crystalline polymer such as PEO is used as the droplet), as crystallization occurs, the crystalline structure typically can occupy the entire droplet space (**Figure 7c**). The crystals are simple small solid particles with well-defined translational symmetry, although crystallization kinetics can be dramatically affected by the small available space and high

interface area. To form a crystal with broken translational symmetry in the nanoconfined crystallization, two conditions are often needed :1) crystallization takes place at the interface, and 2) there is a defined angle between the crystal lattice orientation and the interface, as illustrated in **Figure 7a**. In the PLLA crystalsome case, as previously discussed, the polymer chains (c axis) are perpendicular to the local lamellar surface, hence along the radial direction. The c axis therefore continuously rotates from one location to another, leading to the broken translational symmetry.

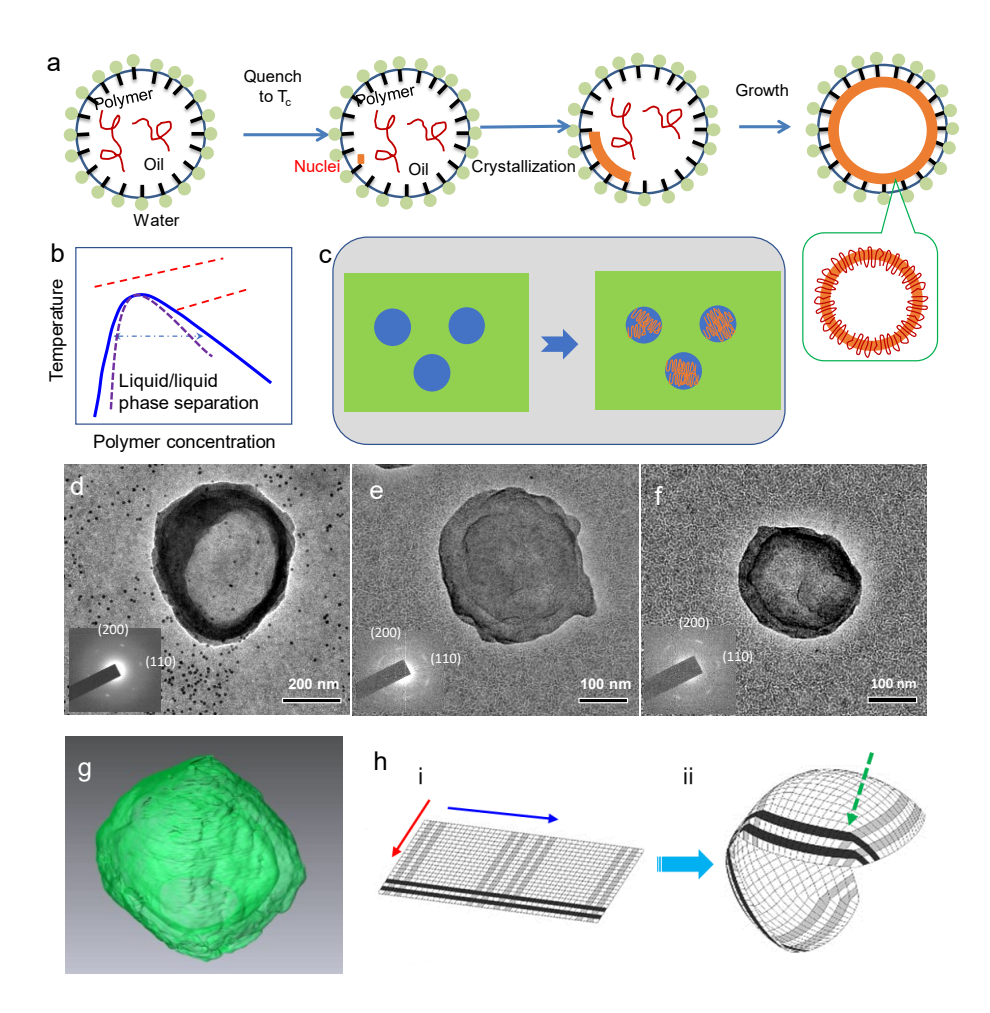


Figure 7. Crystalsomes as shape-translational symmetry incommensurate polymer crystals. (a) schematic representation of the formation process of polymer crystalsome using emulsion solution crystallization. (b) typical crystalline polymer solution phase diagram. To form

crystalsomes, crystallization should be conducted between crystallization line (red dotted line and the binodal). (c) Confined crystallization of liquid droplet. (d-f) TEM images and SAED of crystalsomes with different diameters. (g) reconstructed crystalsome image using TEM tomography.[29] (h) Schematics showing lattice splay on a spherical surface.

Because of the incommensurability between translational symmetry and the curved space, chain packing in crystalsomes is frustrated and the lattice translational symmetry must be broken. Early study of crystallization on a spherical curved surface investigated a colloidal system when monodispersed microparticles are crystallized on a water droplet surface. [78, 79] The structure can be viewed as 2D crystallization on curved space or tiling a crystalline lattice on spherical surface. Curved space incudes ± 1 disclinations, in the particle packing and these disclinations form arrays of high angle grain boundaries that terminate freely within the crystal (Figure 8a,b), termed as "giant scar". In the case of attractive particles on a droplet, isotropic growth occurs to a critical crystal size, above which anisotropic growth takes over producing a ribbon-like appearance on the droplet surface (Figure 8c,d), which is attributed to the elastic strain energy induced by curvature. In polymer crystalsomes, a similar argument can be applied. In PLLA and PE crystalsomes, crystalline structure remains the same compared with those obtained in solution crystallization, indicating that polymer crystalsomes are similar to the attractive particle case and the large voids in Figure 8c therefore can be viewed as defects between better packed crystallites. The crystallite size can be estimated using Scherrer equation based on X-ray diffraction data. Results showed that the crystallite size gradually decreases with the crystalsome diameter, from ~ 22 nm for a flat crystal to ~ 12 nm for 150 nm PLLA crystalsomes calculated from the (200)/(110) reflection peak (Figure 8e). Considering each

crystallite as one building block, for the circumference of a 150nm crystalsome, 40 pieces of crystallites are needed to complete the packing and each domain is ~9° from the adjacent one (**Figure 8f**) and defects have to accumulate between these domains to fulfill this orientational change.

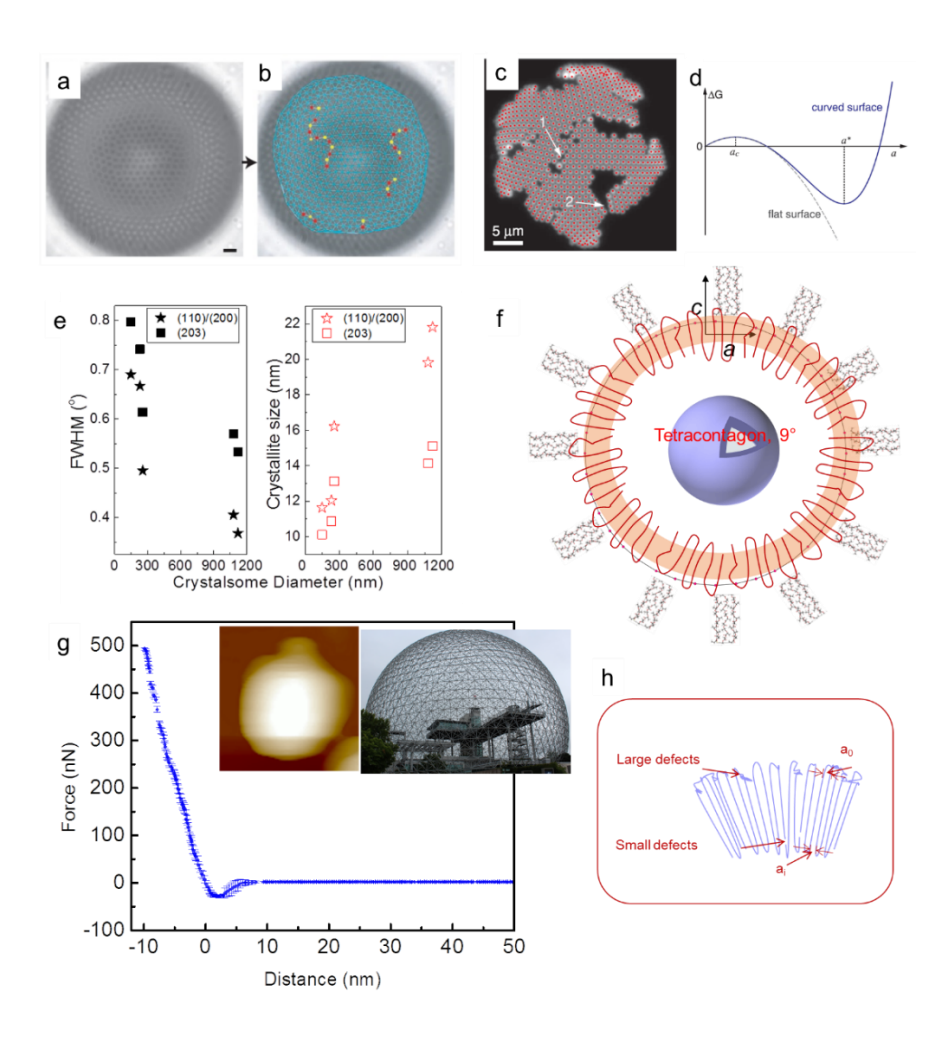


Figure 8. Packing on spherical surface. (a-b) Light microscope image of particle-coated surface and corresponding triangulation pattern with red and yellow dots representing

+1 and -1 disclinations, respectively.[78] (c-d) Attractive particles on a surface (inset) with corresponding free energy diagram for crystal growth on curved and flat surface;[79] (e) Full width of half maximum of (110)/(200) and (203) WAXD diffraction peaks of PLLA

crystalsomes and the corresponding crystallite size. [29] (f) Schematic representation of the chain orientation of the cross-section of a PLLA crystalsome. Note that based on the crystallite size, the equator of the crystalsome can be divided into 40 domains. (g) AFM force-deformation curve of PLLA crystalsome. Inset shows an AFM height image and a photo of a geodesic building. (h) Schematic representation of chain splaying along the radial direction of a crystalsome. [29]

While domain size calculated form Scherrer equation highlights the in-plane defects since (110)/(200) reflections were used for the calculation, defects along the radial direction also exist and play a significant role in crystalsome mechanical properties. AFM indentation experiments showed that the membrane bending modulus of PLLA crystalsomes are orders of magnitude higher than glassy polymersomes with a similar shell thickness (Figure 8g). The structure of PLLA crystalsome mimics typical geodesic buildings (right inset in Figure 8g), which are constituted by units packed in two-dimensional lattices on curved surface and are known for its mechanical stability. Other examples include viral capsids, pollen grains, insect eyes, silica skeletons of unicellular algae. Similar systems have been studied in tiling a spherical surface. Kepler showed that the finite polyhedral with regular polygon faces and all vertices identically surrounded are the five regular polyhedral (the Platonic solids), the 13 Archimedean solids, and the prisms and antiprisms. [80, 81] Euler proposed the Euler characteristic defining the relationship between the numbers of vertices, edges and faces in a given polyhedron. [82] When comparing a polyhedron with the observed crystalsome, two main points can be made: 1) Small crystallite domains mimic polyhedron faces and defects in crystalsome can be viewed as polyhedron edges and vertices. From a crystallization viewpoint, on the molecular level, as polymer chains are perpendicular to the crystalsome surface and there is a finite thickness of the crystalsome shell, polymer chains must splay from the inner to outer surface of

the crystal. Simple calculation shows that the lattice strain associated with the splay can be as high as 14.5% for small crystalsomes (**Figure 8h**). It has been proposed that defect packing along the radial direction could be the key for such large lattice strain: small defects such as vacancies would be arranged near the inner surface while large defect on the outter surface. 2) Note that the crystalsomes are formed at the emulsion droplet surface and slow crystal growth facilitates the unique defect arrangement. The lattice orientation along the spherical surface may not significantly change due to the slow crystallization process. Deep quenching in emulsion crystallization could lead to multiple nucleation events in one droplet, and the lattice orientation between adjacent crystallites might be uncorrelated.

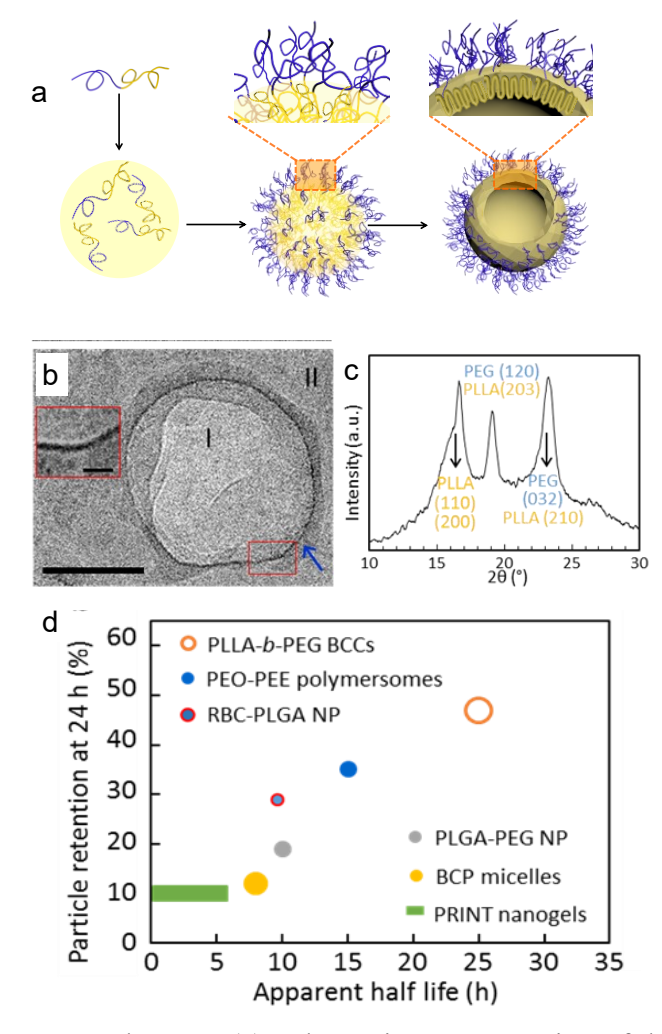


Figure 9. Block copolymer crystalsomes. (a) Schematic representation of the formation of PLLA-b-PEO BCC. (b) a cryo-TEM image and (c) WAXD pattern of the BBC. (d) highlights the superb long circulation time for the newly formed BCCs.[34]

Block copolymer crystalsomes (BCCs) were also reported where amphiphilic PLLA-b-PEO was used as the surfactant to form emulsion droplets.[34] Slow cooling of the emulsion system allows PLLA to crystallize while PEO is solvated in water to stabilize the emulsion (**Figure 9a**). **Figure 9b** shows a cryo-TEM image of the BCCs and PLLA crystal structure was confirmed using WAXD (**Figure 9c**) as well as SAED experiments. Since BCCs have similar

spherical shape and size, similar translational symmetry breaking argument as previously discussed can be applied here. In BCCs, the thickness of PLLA lamellae was found to be small, leading to a mild lattice strain compared to thicker homopolymer crystalsomes. The PEO brushes on the surface of the BCCs also renders the structure water dispersible. Preliminary study shows that this unique structure has a ultralong blood circulation life (**Figure 9d**) compared with other nanoparticle carriers and this superb performance was attributed to the combination of excellent mechanical stability and uniform PEO brush of the BCCs.

Conclusion

In this article, we discussed polymer crystalline morphology from the viewpoint of unit cell and translational symmetry. We used SSC and SSIC to describe reported single crystal level morphologies. For SSC, in addition to classical lamellar crystals, a few unconventional morphologies were discussed. Non-flat single crystals such as helicoidal, scrolled and spherical crystals were presented as SSICs because the non-flat morphology is incommensurate with translational symmetry in Euclidean space. While helicoidal and scrolled single crystals have been extensively studied, spherical crystals such as crystalsomes have only been recently discovered. Formation, structure and chain packing in polymer crystalsomes were discussed. Although in the early stage of development, intriguing mechanical and biomedical properties have already been reported for crystalsomes. We anticipate that shape-translational symmetry commensurability provides a unique framework to study polymer crystals and related self-assembly structures.

Acknowledgements

This work was partially supported by the National Science Foundation Grant DMR 1709136, CHE 1709119, and CMMI 1762626.

References

- [1] B. Wunderlich, Macromolecular Physics Vol. 1: Crystal Structure, Morphology, Defects, Academic Press, New York, 1973.
- [2] B. Wunderlich, Macromolecular Physics Vol 2: Crystal Nucleation, Growth, Annealing, Academic Press, New York, 1976.
- [3] B. Wunderlich, Macromolecular Physics Vol 3: Crystal Melting, Academic Press, New York, 1980.
- [4] P. Geil, Polymer Single Crystals, Robert Krieger Pub., Huntington, N. Y., 1973.
- [5] L. Mandelkern, Crystallization of Polymers Vol. 2: Kinetics and Mechanisms, Cambridge University Press, Cambridge, 2004.
- [6] L. Mandelkern, Crystallization of Polymers Vol 1: Equilibrium Concepts, Cambridge University Press, Cambridge, 2004.
- [7] A. Keller, S.Z.D. Cheng, The role of metastability in polymer phase transitions, Polymer 39 (1998) 4461-4487.
- [8] B. Lotz, T. Miyoshi, S.Z. Cheng, 50th Anniversary Perspective: Polymer Crystals and Crystallization: Personal Journeys in a Challenging Research Field, Macromolecules 50 (2017) 5995-6025.
- [9] S.Z.D. Cheng, Phase Transitions in Polymers, the Role of Metastable States, Elsevier2008.
- [10] G. Reiter, G.R. Strobl, Progress in understanding of polymer crystallization, Springer2007.
- [11] R.M. Michell, A.J. Muller, Confined crystallization of polymeric materials, Prog. Polym. Sci. 54-55 (2016) 183-213.
- [12] G. Strobl, Crystallization and melting of bulk polymers: New observations, conclusions and a thermodynamic scheme, Prog. Polym. Sci. 31 (2006) 398-442.

- [13] Y. Furushima, C. Schick, A. Toda, Crystallization, recrystallization, and melting of polymer crystals on heating and cooling examined with fast scanning calorimetry, Polymer Crystallization 1 (2018) e10005.
- [14] Z.M. Hudson, C.E. Boott, M.E. Robinson, P.A. Rupar, M.A. Winnik, I. Manners, Tailored hierarchical micelle architectures using living crystallization-driven self-assembly in two dimensions, Nature Chemistry 6 (2014) 893.
- [15] M. Inam, G. Cambridge, A. Pitto-Barry, Z.P.L. Laker, N.R. Wilson, R.T. Mathers, A.P. Dove, R.K. O'Reilly, 1D vs. 2D shape selectivity in the crystallization-driven self-assembly of polylactide block copolymers, Chem. Sci. 8 (2017) 4223-4230.
- [16] J. Xu, Y. Ma, W. Hu, M. Rehahn, G. Reiter, Cloning polymer single crystals through self-seeding, Nat. Mater. 8 (2009) 348-353.
- [17] B. Li, C.Y. Li, Immobilizing Au nanoparticles with polymer single crystals, patterning and asymmetric functionalization, J. Am. Chem. Soc. 129 (2007) 12-13.
- [18] B. Li, B.B. Wang, R.C.M. Ferrier, C.Y. Li, Programmable Nanoparticle Assembly via Polymer Single Crystals, Macromolecules 42 (2009) 9394-9399.
- [19] B. Dong, B. Li, C.Y. Li, Janus nanoparticle dimers and chains via polymer single crystals, J. Mater. Chem. 21 (2011) 13155-13158.
- [20] B. Dong, D.L. Miller, C.Y. Li, Polymer Single Crystal As Magnetically Recoverable Support for Nanocatalysts, J. Phys. Chem. Lett. 3 (2012) 1346-1350.
- [21] B. Dong, W. Wang, D.L. Miller, C.Y. Li, Polymer-single-crystal@nanoparticle nanosandwich for surface enhanced Raman spectroscopy, J. Mater. Chem. 22 (2012) 15526-15529.
- [22] B. Dong, T. Zhou, H. Zhang, C.Y. Li, Directed Self-Assembly of Nanoparticles for Nanomotors, ACS Nano 7 (2013) 5192-5198.
- [23] H. Qi, T. Zhou, S. Mei, X. Chen, C.Y. Li, Responsive Shape Change of Sub-5 nm Thin, Janus Polymer Nanoplates, ACS Macro. Lett. 5 (2016) 651-655.
- [24] E.D. Laird, C.Y. Li, Structure and Morphology Control in Crystalline-Polymer/Carbon-Nanotube Composites, Macromolecules 46 (2013) 2877-2891.
- [25] T. Zhou, B. Dong, H. Qi, H.K. Lau, C.Y. Li, One-step formation of responsive "dumbbell" nanoparticle dimers via quasi-two-dimensional polymer single crystals, Nanoscale 6 (2014) 4551-4554.

- [26] S. Mei, M. Staub, C.Y. Li, Directed Nanoparticle Assembly through Polymer Crystallization, Chemistry—A European Journal 26 (2020) 349-361.
- [27] C.Y. Li, Polymer single crystal meets nanoparticles, J. Poly. Sci. Poly. Phys. 47 (2009) 2436-2440.
- [28] H. Qi, W. Wang, C.Y. Li, Janus Polymer Single Crystal via Evaporative Crystallization, ACS Macro. Lett. 3 (2014) 675-678.
- [29] W. Wang, H. Qi, T. Zhou, S. Mei, L. Han, T. Higuchi, H. Jinnai, C.Y. Li, Highly robust crystalsome via directed polymer crystallization at curved liquid/liquid interface, Nat. Commun. 7 (2016) 10599.
- [30] P. Schaaf, B. Lotz, J.C. Wittmann, Liquid-liquid phase separation and crystallization in binary polymer systems, Polymer 28 (1987) 193-200.
- [31] M.C. Staub, C.Y. Li, Confined and Directed Polymer Crystallization at Curved Liquid/Liquid Interface, Macromol. Chem. Phys. 219 (2018) 1700455.
- [32] M.C. Staub, C.Y. Li, Polymer crystallization at liquid liquid interface, Polymer Crystallization 1 (2018) 10045.
- [33] W. Wang, M.C. Staub, T. Zhou, D.M. Smith, H. Qi, E.D. Laird, S. Cheng, C.Y. Li, Polyethylene nano crystalsomes formed at a curved liquid/liquid interface, Nanoscale 10 (2018) 268-276.
- [34] H. Qi, H. Zhou, Q. Tang, J.Y. Lee, Z. Fan, S. Kim, M.C. Staub, T. Zhou, S. Mei, L. Han, D.J. Pochan, H. Cheng, W. Hu, C.Y. Li, Block copolymer crystalsomes with an ultrathin shell to extend blood circulation time, Nat. Commun. 9 (2018) 3005.
- [35] J. Wittmann, B. Lotz, Polymer decoration: the orientation of polymer folds as revealed by the crystallization of polymer vapors, J. Poly. Sci., Poly. Phy. 23 (1985) 205-226.
- [36] A. Toda, M. Okamura, M. Hikosaka, Y. Nakagawa, Three-dimensional shape of polyethylene single crystals grown from dilute solutions and from the melt, Polymer 46 (2005) 8708-8716.
- [37] N. Grozev, I. Botiz, G. Reiter, Morphological instabilities of polymer crystals, Eur. Phys. J. E. 27 (2008) 63-71.
- [38] G. Reiter, Some unique features of polymer crystallisation, Chem. Soc. Rev. 43 (2014) 2055-2065.

- [39] J. Wittmann, B. Lotz, Epitaxial crystallization of polymers on organic and polymeric substrates, Prog. Polym. Sci. 15 (1990) 909-948.
- [40] H. Li, S. Yan, Surface-induced polymer crystallization and the resultant structures and morphologies, Macromolecules 44 (2011) 417-428.
- [41] S. Mei, H. Qi, T. Zhou, C.Y. Li, Precisely Assembled Cyclic Gold Nanoparticle Frames by 2D Polymer Single-Crystal Templating, Angew. Chem. Inter. Ed. 56 (2017) 13645-13649.
- [42] T. Zhou, H. Qi, L. Han, D. Barbash, C.Y. Li, Towards controlled polymer brushes via a self-assembly-assisted-grafting-to approach, Nat. Commun. 7 (2016) 11119.
- [43] T. Zhou, B. Han, H. Qi, Q. Pan, D.M. Smith, L. Han, C.Y. Li, Velcro-mimicking surface based on polymer loop brushes, Nanoscale 10 (2018) 18269-18274.
- [44] S. Mei, C.Y. Li, Terraced and Smooth Gradient Polymer Brushes via a Polymer-Single-Crystal-Assisted-Grafting-To Method, Angew. Chem. Int. Ed. 57 (2018) 15758-15761.
- [45] X. Wang, G. Guerin, H. Wang, Y. Wang, I. Manners, M.A. Winnik, Cylindrical block copolymer micelles and co-micelles of controlled length and architecture, Science 317 (2007) 644-647.
- [46] H. Qiu, Y. Gao, C.E. Boott, O.E. Gould, R.L. Harniman, M.J. Miles, S.E. Webb, M.A. Winnik, I. Manners, Uniform patchy and hollow rectangular platelet micelles from crystallizable polymer blends, Science 352 (2016) 697-701.
- [47] C.Y. Li, L. Li, W. Cai, S.L. Kodjie, K.K. Tenneti, Nanohybrid shish-kebabs: periodically functionalized carbon nanotubes, Adv. Mater. 17 (2005) 1198-1202.
- [48] L. Li, C.Y. Li, C.Y. Ni, Polymer crystallization-driven, periodic patterning on carbon nanotubes, J. Am. Chem. Soc. 128 (2006) 1692-1699.
- [49] W. Wang, C.Y. Li, Single-Walled Carbon Nanotube-Induced Orthogonal Growth of Polyethylene Single Crystals at a Curved Liquid/Liquid Interface, ACS Macro. Lett. 3 (2014) 175-179.
- [50] E.D. Laird, H. Qi, C.Y. Li, Water nanocondensation on polymer single crystal-decorated buckypaper, Polymer 70 (2015) 271-277.
- [51] W. Wang, Z. Huang, E.D. Laird, S. Wang, C.Y. Li, Single-walled carbon nanotube nanoring induces polymer crystallization at liquid/liquid interface, Polymer 59 (2015) 1-9.
- [52] B. Li, L.Y. Li, B.B. Wang, C.Y. Li, Alternating patterns on single-walled carbon nanotubes, Nature Nanotech. 4 (2009) 358-362.

- [53] B.B. Wang, B. Li, J. Xiong, C.Y. Li, Hierarchically Ordered Polymer Nanofibers via Electrospinning and Controlled Polymer Crystallization, Macromolecules 41 (2008) 9516-9521.
- [54] X. Chen, B. Dong, B.B. Wang, R. Shah, C.Y. Li, Crystalline Block Copolymer Decorated, Hierarchically Ordered Polymer Nanofibers, Macromolecules 43 (2010) 9918-9927.
- [55] X. Chen, W. Wang, S. Cheng, B. Dong, C.Y. Li, Mimicking Bone Nanostructure by Combining Block Copolymer Self-Assembly and 1D Crystal Nucleation, ACS Nano 7 (2013) 8251-8257.
- [56] X. Chen, S.E. Gleeson, T. Yu, N. Khan, R.W. Yucha, M. Marcolongo, C.Y. Li, Hierarchically ordered polymer nanofiber shish kebabs as a bone scaffold material, J. Biomed. Mater. Res. A 105 (2017) 1786-1798.
- [57] Q. Xie, X. Chang, Q. Qian, P. Pan, C.Y. Li, Structure and Morphology of Poly (lactic acid) Stereocomplex Nanofiber Shish Kebabs, ACS Macro. Lett. 9 (2020) 103-107.
- [58] A.C. Attia, T. Yu, S.E. Gleeson, M. Petrovic, C.Y. Li, M. Marcolongo, A review of nanofiber shish kebabs and their potential in creating effective biomimetic bone scaffolds, Regenerative Engineering and Translational Medicine 4 (2018) 107-119.
- [59] T. Yu, S.E. Gleeson, C.Y. Li, M. Marcolongo, Electrospun poly (ε caprolactone) nanofiber shish kebabs mimic mineralized bony surface features, J. Biomed. Mater. Res. B 107 (2019) 1141-1149.
- [60] B. Lotz, S.Z.D. Cheng, A critical assessment of unbalanced surface stresses as the mechanical origin of twisting and scrolling of polymer crystals, Polymer 46 (2005) 577-610.
- [61] A.J. Lovinger, Twisted Crystals and the Origin of Banding in Spherulites of Semicrystalline Polymers, Macromolecules 53 (2020) 741-745.
- [62] D. Bassett, A. Hodge, On lamellar organization in banded spherulites of polyethylene, Polymer 19 (1978) 469-472.
- [63] J.M. Schultz, Self-induced field model for crystal twisting in spherulites, Polymer 44 (2003) 433-441.
- [64] T. Kyu, H.-W. Chiu, A. Guenthner, Y. Okabe, H. Saito, T. Inoue, Rhythmic growth of target and spiral spherulites of crystalline polymer blends, Phys. Rev. Lett. 83 (1999) 2749.
- [65] M. Rosenthal, G. Bar, M. Burghammer, D.A. Ivanov, On the nature of chirality imparted to achiral polymers by the crystallization process, Angew. Chem. Int. Ed. 50 (2011) 8881-8885.

- [66] C.Y. Li, S.Z.D. Cheng, J.J. Ge, F. Bai, J.Z. Zhang, I.K. Mann, F.W. Harris, L.C. Chien, D.H. Yan, T.B. He, B. Lotz, Double twist in helical polymer "soft" crystals, Phys. Rev. Lett. 83 (1999) 4558-4561.
- [67] C.Y. Li, S.Z.D. Cheng, J.J. Ge, F. Bai, J.Z. Zhang, I.K. Mann, L.C. Chien, F.W. Harris, B. Lotz, Molecular orientations in flat-elongated and helical lamellar crystals of a main-chain nonracemic chiral polyester, J. Am. Chem. Soc. 122 (2000) 72-79.
- [68] C.Y. Li, S.Z.D. Cheng, X. Weng, J.J. Ge, F. Bai, J.Z. Zhang, B.H. Calhoun, F.W. Harris, L.C. Chien, B. Lotz, Left or right, it is a matter of one methylene unit, J. Am. Chem. Soc. 123 (2001) 2462-2463.
- [69] C.Y. Li, J.J. Ge, F. Bai, B.H. Calhoun, F.W. Harris, S.Z.D. Cheng, L.C. Chien, B. Lotz, H.D. Keith, Early-stage formation of helical single crystals and their confined growth in thin film, Macromolecules 34 (2001) 3634-3641.
- [70] C.Y. Li, D.H. Yan, S.Z.D. Cheng, F. Bai, J.J. Ge, B.H. Calhoun, T.B. He, L.C. Chien, F.W. Harris, B. Lotz, Helical single-lamellar crystals thermotropically formed in a synthetic nonracemic chiral main-chain polyester, Physical Review B 60 (1999) 12675-12680.
- [71] C.Y. Li, S. Jin, X. Weng, J.J. Ge, D. Zhang, F. Bai, F.W. Harris, S.Z.D. Cheng, D.H. Yan, T.B. He, B. Lotz, L.C. Chien, Liquid crystalline phases, microtwinning in crystals and helical chirality transformations in a main-chain chiral liquid crystalline polyester, Macromolecules 35 (2002) 5475-5482.
- [72] X. Weng, C.Y. Li, S. Jin, D. Zhang, J.Z. Zhang, F. Bai, F.W. Harris, S.Z.D. Cheng, Helical twist senses, liquid crystalline behavior, crystal microtwins, and rotation twins in a polyester containing main-chain molecular asymmetry and effects of the number of methylene units in the backbones on the phase structures and morphologies of its homologues, Macromolecules 35 (2002) 9678-9686.
- [73] W. Cai, C.Y. Li, L. Li, B. Lotz, M. Keating, D. Marks, Sub-micro tube/scroll polymer single crystal from Nylon 6,6, Adv. Mater. 16 (2004) 600-605.
- [74] B. Lotz, S. Cheng, C. Li, Structure of Negative Spherulites of Even–Even Polyamides. Introducing a Complex Multicomponent Spherulite Architecture, Macromolecules 51 (2018) 5138-5156.

- [75] B. Lotz, Analysis and Observation of Polymer Crystal Structures at the IndividualStem Level, in: G. Allegra (Ed.), Interphases and Mesophases in Polymer Crystallization I, Springer Berlin Heidelberg, Berlin, Heidelberg, 2005, pp. 17-44.
- [76] G.R. Burks, H. Qi, S.E. Gleeson, S. Mei, C.Y. Li, Structure and Morphology of Poly (vinylidene fluoride) Nanoscrolls, ACS Macro. Lett. 7 (2017) 75-79.
- [77] H. Xiong, C.-K. Chen, K. Lee, R.M. Van Horn, Z. Liu, B. Ren, R.P. Quirk, E.L. Thomas, B. Lotz, R.-M. Ho, Scrolled polymer single crystals driven by unbalanced surface stresses: rational design and experimental evidence, Macromolecules 44 (2011) 7758-7766.
- [78] A.R. Bausch, M.J. Bowick, A. Cacciuto, A.D. Dinsmore, M.F. Hsu, D.R. Nelson, M.G. Nikolaides, A. Travesset, D.A. Weitz, Grain boundary scars and spherical crystallography, Science 299 (2003) 1716-1718.
- [79] G. Meng, J. Paulose, D.R. Nelson, V.N. Manoharan, Elastic Instability of a Crystal Growing on a Curved Surface, Science 343 (2014) 634-637.
- [80] E.A. Lord, A.L. Mackay, S. Ranganathan, New Geometries for New Materials, Cambridge University Press, Cambridge, 2006.
- [81] P.R. Cromwell, Polyhedra, Cambridge University Press, Cambridge, 1999.
- [82] L. Euler, Elementa doctrinae solidorum, Scholarly Commons1758.

Biography

Mark Staub received his B.S. degree in Chemistry from Gettysburg College. He then joined Becton Dickinson as a Scientist II in their Diagnostic Systems analytical lab. Currently, he is completing a Ph.D. in Materials Science and Engineering under the direction of Dr. Christopher Li. His research involves directing polymer crystallization to obtain unique nanostructures that give fundamental insight into ordering processes in polymeric systems, while showing potential in a variety of applications.



Christopher Li is a Professor in the Department of Materials Science and Engineering at Drexel University. He received his B.S. degree in Polymer Chemistry from the University of Science and Technology of China in 1995 and his Ph.D. in Polymer Science from the University of Akron in 1999. His research interests center on the structure and morphology of polymers and soft materials. He is a Fellow of the American Physical Society the North American Thermal Analysis Society.

